© 2017. Published by The Company of Biologists Ltd | Journal of Experimental Biology (2017) 220, 478-486 doi:10.1242/jeb.148312

RESEARCH ARTICLE

Increasing trunk flexion transforms human leg function into that of birds despite different leg morphology

Soran Aminiaghdam*, Christian Rode, Roy Müller and Reinhard Blickhan

ABSTRACT

Pronograde trunk orientation in small birds causes prominent intra-limb asymmetries in the leg function. As yet, it is not clear whether these asymmetries induced by the trunk reflect general constraints on the leg function regardless of the specific leg architecture or size of the species. To address this, we instructed 12 human volunteers to walk at a self-selected velocity with four postures: regular erect, or with 30 deg, 50 deg and maximal trunk flexion. In addition, we simulated the axial leg force (along the line connecting hip and centre of pressure) using two simple models: spring and damper in series, and parallel spring and damper. As trunk flexion increases, lower limb joints become more flexed during stance. Similar to birds, the associated posterior shift of the hip relative to the centre of mass leads to a shorter leg at toe-off than at touchdown, and to a flatter angle of attack and a steeper leg angle at toe-off. Furthermore, walking with maximal trunk flexion induces right-skewed vertical and horizontal ground reaction force profiles comparable to those in birds. Interestingly, the spring and damper in series model provides a superior prediction of the axial leg force across trunk–flexed gaits compared with the parallel spring and damper model; in regular erect gait, the damper does not substantially improve the reproduction of the human axial leg force. In conclusion, mimicking the pronograde locomotion of birds by bending the trunk forward in humans causes a leg function similar to that of birds despite the different morphology of the segmented legs.

KEY WORDS: Trunk orientation, Asymmetry, Able-bodied walking, Posture, Leg model

INTRODUCTION

Bipedal walking and running are the common human gaits. Humans, birds, and sometimes apes and monkeys use bipedal locomotion (Alexander, 2004; Hirasaki et al., 2004). In contrast to most animals, human walking is characterized by an erect trunk (Grasso et al., 2000), extended limbs during the stance phase (Foster et al., 2013) and two-peaked vertical ground reaction force (GRF) patterns (Alexander, 2004; Winiarski and Rutkowska-Kucharska, 2009; Toda et al., 2015). The dynamics of locomotion can be affected by altering specific gait requirements. For example, running with flexed knee decreases the vertical stiffness of the legs relative to normal human running (McMahon et al., 1987).

Although bipedal locomotion in birds and humans seems to be highly adapted (Alexander, 2004; Müller et al., 2016), the design of their locomotor systems is drastically different, not only in terms of segmentation but also for their hip placement with respect to the centre of mass (CoM) (Gatesy and Biewener, 1991). Unlike human CoM, which is situated above the hip, owing to a horizontal upper body orientation (pronograde) in birds, the hip is located posterior to the CoM (Hutchinson and Allen, 2009). Birds with horizontal trunk orientation achieve steady-state locomotion using two leg strategies (throughout the article, 'leg' refers to the segment connecting the hip and the centre of pressure, CoP). The first is a kinematic asymmetry, i.e. longer legs at touchdown (TD) and shorter legs at toe-off (TO); the second is a kinetic asymmetry i.e. exertion of greater forces in the early stance phase and attenuated forces during the rest of stance phase (a right-skewed GRF pattern) (Andrada et al., 2014).

The human trunk accounts for more than 50% of total body mass; hence, trunk orientation has a significant effect on the position of the CoM and human locomotion (de Leva, 1996; Gillet et al., 2003; Leteneur et al., 2009). The trunk stabilization, basically the task of balancing an unstable inverted pendulum standing on the hip (Maus et al., 2010), is an important task in human locomotion. Humans are able to adopt pitched positions on command, but certainly, our locomotor system is not tuned to such postures. This ability can be exploited in experiments using different postures to shed new light on how trunk orientation can influence the leg function or on the biomechanically unfavourable, probably metabolically expensive, posterior position of the hip with respect to the upper body CoM in birds (Alexander, 1991; Blickhan et al., 2015).

Despite the different morphology of human and bird legs, in both walking and running, the function of the virtual leg can be described with surprisingly simple phenomenological gait models (Maus et al., 2010; Andrada et al., 2014). In a system including a trunk with inertia, the human leg function could be approximated with a spring-like telescopic leg and hip torques that keep the trunk upright (Maus et al., 2010). A spring-like axial leg function may result from compliant muscles and properly adjusted muscle activation (Geyer et al., 2003). However, when modelling the pronograde locomotion of birds, the spring describing the compliant axial leg function (leg length and force in leg direction) was complemented by axial damping to successfully explain the axial kinetic and kinematic asymmetries induced by trunk orientation (Andrada et al., 2014).

Following the principle of parsimony, it is important to find simple yet well-fitting models of the leg function because they are convenient and transparent in systematic studies on the influence of basic parameters on performance. Moreover, such models can be applied to the investigation of the locomotion stability (Geyer et al., 2006; Maus et al., 2010; Andrada et al., 2014) or in virtual model control of complex machines (Sreenath et al., 2011). Dissimilar leg models may yield different predictions with respect to gait stability. Although it is common to use a spring and a damper in parallel to describe the axial leg function (Shen and Seipel, 2012; Andrada et al., 2014), to the best of our knowledge, a model with a damper in series with a spring using the same number of parameters has not yet been employed to investigate the asymmetric axial leg function.

Department of Motion Science, Institute of Sport Sciences, Friedrich Schiller University Jena, Seidelstraße 20, Jena 07740, Germany.

*Author for correspondence (soran.aminiaghdam@uni-jena.de)

S.A., 0000-0001-9310-6768

Received 14 August 2016; Accepted 17 November 2016

Journal of Experimental Biology

Journal of Experimental Biology (2017) 220, 478-486 doi:10.1242/jeb.148312

List of symbols and abbreviations

α_{TD}, α_{TO}	leg orientation at touchdown and at toe-off
BW	body weight
CoM	centre of mass
CoP	centre of pressure
c_p, c_s	damping parameter (parallel spring and serial spring)
F_a	axial force
GRF	ground reaction force
H_{GRFb}, H_{GRFp}	peak horizontal force (braking and propulsive)
I_S	vertical or support impulses
k_p, k_s	stiffness parameter (parallel spring and serial spring)
L	instantaneous leg length
l_0	rest length of the leg
l_d, l_{s0}	rest length (serial damper and serial spring)
$\dot{l}$, $\dot{l}_d$	rate of length change (leg and serial damper)
PSD	parallel-spring damper
RE	regular erect trunk alignment
RMS	root mean square
SSD	series-spring damper
TD, TO	touchdown, toe-off
TF1	30 deg of trunk flexion
TF2	50 deg of trunk flexion
TF3	maximal trunk flexion
V_{GRF1}, V_{GRF2}	vertical ground reaction force (first and second peak)

Gait asymmetries are the key traits of human locomotion (Dingwell et al., 2010). This is evident in a left–right asymmetrical behaviour during locomotion in able-bodied participants, even with equal leg masses (Sadeghi et al., 2000), in temporal and kinematic parameters (Gundersen et al., 1989), in GRF (Herzog et al., 1989) and in joint moments (Leteneur et al., 2009). While such inter-limb asymmetries have been extensively studied in human walking and also in technical walking systems (e.g. legged robots, prosthetic legs) (Merker et al., 2011), the intra-limb asymmetries in leg function are not well understood. In spite of a considerable number of studies on the potential effect of trunk posture on the human walkers whether as an imposed trunk posture (Grasso et al., 2000; Saha et al., 2008; Kluger et al., 2014), the natural inclination of the trunk (Leteneur et al., 2009, 2013) or age-related flexed posture (McGibbon and Krebs, 2001; de Groot et al., 2014), little is known about the effects of trunk orientation on the axial leg function, specifically when trunk posture is varied across a wide range of angles in the sagittal plane.

We hypothesize that humans increasingly approximate asymmetries observed in the axial leg function of birds during the stance phase, characterized by a right-skewed GRF profile and increased TD and TO kinematic asymmetries when proceeding from the orthograde to pronograde trunk orientation. This would indicate that the trunk posture imposes specific constraints on bipedal terrestrial locomotion in terms of leg function despite considerable differences in the detailed morphology of the leg or the size of the biological systems. We test this hypothesis in able-bodied participants walking with various trunk orientations. Furthermore, we investigate whether either leg model, the parallel spring and damper system or the model with spring and damper in series, gives a superior prediction of the axial leg function.

MATERIALS AND METHODS

Human subjects

Twelve able-bodied adults (six females, six male) aged 26±3.35 years (mean±s.d.) with average height of 169.75±7.41 cm and average mass of 65.08±8.07 kg participated in this study. Participants had no known musculoskeletal or neurological disorders that could affect their walking pattern or trunk motion. An informed consent form was signed by each participant before participation. The experimental protocol was approved by the local Ethics Committee of the University of Jena (3532-08/12) and carried out according to the Declaration of Helsinki.

Instrumentation

Data collection was conducted at the Biomechanics Laboratory at the Sports Institute within University of Jena. All trials were recorded with eight cameras (240 Hz) by a 3D infrared system (MCU1000, Qualisys, Gothenburg, Sweden) and synchronized with force acquisition by using the trigger of the Kistler software and hardware. Three consecutive force platforms (9285BA, 9281B, 9287BA; Kistler, Winterthur, Switzerland) embedded in the middle portion of a 12 m walkway sampled force at 1000 Hz.

A 13 body segment model was defined by 21 markers (spherical retro-reflective surface, 14 mm). The markers were placed on the following bony landmarks: fifth metatarsal heads, lateral malleoli, lateral epicondyles of femurs, greater trochanters, anterior superior iliac spines, posterior superior iliac spines, L5–S1 junction, lateral humeral epicondyles, wrists, acromioclavicular joints, seventh cervical spinous process and middle of the forehead.

Procedure

Participants were asked to walk at self-selected normal walking speed for each of the four conditions: with their regular erect trunk alignment (RE), with 30 deg of trunk flexion (TF1), with 50 deg of trunk flexion (TF2), and with maximal trunk flexion (TF3) (Fig. 1, Fig. 2A). To produce the most consistent trunk posture across participants, trunk flexion was achieved by bending from the hips (Saha et al., 2008). Considering this criterion, the TF3 constituted the maximum amount of trunk flexion that the participants could sustain while walking. Trunk angle was defined by the angle sustained by the line connecting the midpoint between the L5–S1 junction (L5) and the seventh cervical spinous process (C7) with respect to the vertical (Fig. 1A) (Müller et al., 2014). Practice trials were permitted to allow participants to accommodate to the locomotion conditions and secure step onto the force plates in left–right–left sequence. Trunk angles were compared visually with adjustable-height cardboard templates by a second examiner prior to performing of each trial and during gait along the walkway for TF1 and TF2. For TF3, there was no comparison. The templates, drawn with angles displaying target trunk flexion angles TF1 and TF2, were hung on a wall parallel to the walkway: one at the beginning and the other one in the middle of walkway. The participants accomplished eight trials per condition in which each foot stepped on a single force plate.

Selected variables and parameters

Gait parameters comprised velocity, stance time, step length, swing time and cadence. We determined the mean angles of trunk, hip, knee and ankle throughout the gait cycle (Fig. 1A). The vertical displacement of CoM was determined by body segmental analysis using the anthropometric tables of Zatsiorsky–Seluyanov modified by De Leva relative to the laboratory coordinate system throughout the stance phase (de Leva, 1996; Gard et al., 2004). Related parameters were the values of the kinematic variables at the instants of TD and TO, their range of motion, and their maximal values (ankle: dorsiflexion and plantarflexion).

We assessed the first peak of the vertical ground reaction force (V_{GRF1}), the second peak of the vertical ground reaction force (V_{GRF2}), the peak horizontal braking force (H_{GRFb}) and the peak

Journal of Experimental Biology (2017) 220, 478-486 doi:10.1242/jeb.148312

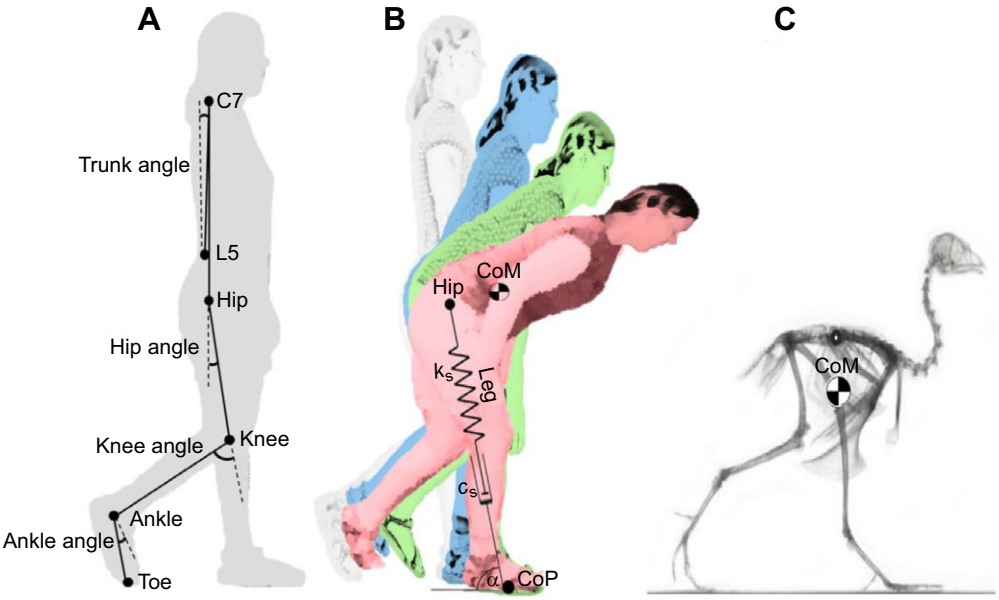

Fig. 1. Human and bird locomotion. (A) Illustration of the definitions of hip, knee and ankle joints as used in this study. (B) Side view of one participant while adopting regular erect (RE, grey), 30 deg trunk flexion (TF1, blue), 50 deg trunk flexion (TF2, green), maximal trunk flexion (TF3, red) postures during level walking gaits and modelling asymmetric leg function as spring and damper in series (SSD). CoM, centre of mass; k_s, stiffness parameter of serial spring; c_s, damping parameter of serial spring; α, leg orientation; CoP, centre of pressure. Consent to publish images was obtained. (C) Lateral X-ray projection of a quail enlarged for comparison (courtesy of Prof. Martin S. Fischer, Institute of Systematic Zoology and Evolutionary Biology with Phyletic Museum, Friedrich Schiller University Jena).

horizontal propulsive force (H_{GRFp}). For kinetic analysis, GRF was normalized to the participant body weight (BW). A vertical GRF threshold of 0.03 BW was used to determine the instants of TD and TO at each contact. Furthermore, we determined the duration of the braking phase relative to the duration of the stance time and calculated the vertical or support impulses (I_S) by integrating the according force–time curves and the normalized I_S to the product of body weight and the square root of the quotient of leg length and gravity (Hof, 1996). Leg (Fig. 1B) was normalized to the distance between the greater trochanter marker and the lateral malleoli marker at the instant of TD. Leg orientation, angle between leg and ground, at the instants of TD (α_{TD}, angle of attack) and TO (α_{TO}) was calculated with respect to the negative *x*-axis (Fig. 1B).

Data processing and statistics

Kinetic and kinematic data of all successful trials were analysed using custom written MATLAB (MathWorks) code. The raw coordinate data were filtered using a fourth-order low-pass, zero-lag Butterworth filter with 12 Hz cut-off frequency.

The effects of trunk orientation on joint kinematics and kinetics were evaluated using SPSS (SPSS Inc., Chicago, IL) with a statistical significance level of 0.05. For all participants, eight trials were analysed for each trunk posture. The data were categorized based on the trunk posture (RE, TF1, TF2 and TF3). Prior to analysis Levene's test and Kolmogorov–Smirnov test were performed to examine the equality of variance and normality of distribution, respectively. If data were parametric, a one-way ANOVA and paired *t*-test were used to examine the differences across gait conditions and in case of a significant difference, *post hoc* Bonferroni testing was employed; otherwise, a Wilcoxon signed-rank test was performed.

Leg models

To determine the axial leg function (Andrada et al., 2014), the sagittal plane GRF of the leg was projected onto the leg axis. Axial leg force was modelled in two different ways: parallel spring and damper elements (PSD), and spring and damper elements in series (SSD) (Fig. 1B). For the parallel arrangement, the axial force F_a is

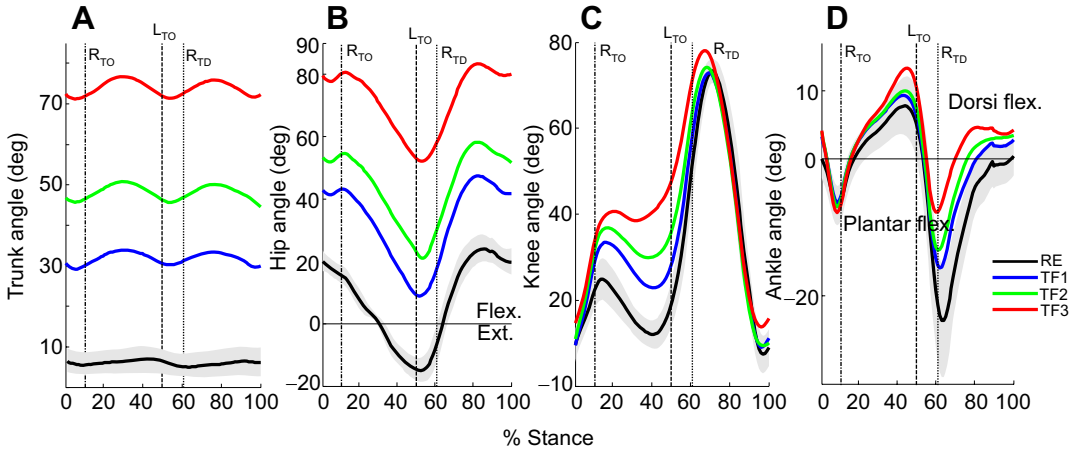

Fig. 2. Trunk and lower limb kinematics. Averaged (A) trunk, (B) hip, (C) knee and (D) ankle angles pertaining to the left limb in the sagittal plane during the gait cycle for RE (black), TF1 (blue), TF2 (green) and TF3 (red) level walking gaits (*N*=12). The grey shaded area represents s.d. of RE gait. RE, regular erect trunk; TF1, 30 deg trunk flexion; TF2, 50 deg trunk flexion; TF3, maximal trunk flexion; R_{TO}, right toe-off; R_{TD}, right touchdown; L_{TO}, left toe-off.

Journal of Experimental Biology

Table 1. Spatiotemporal gait parameters

	RE	TF1	TF2	TF3
Velocity (m s^{-1})	1.49±0.10	1.60±0.12[a]	1.65±0.13[a]	1.63±0.14[a]
Stance time (s)	0.60±0.04	0.57±0.05[a]	0.54±0.04[a,b]	0.54±0.04[a,b]
Swing time (s)	0.40±0.01	0.39±0.03[a]	0.38±0.02[a]	0.38±0.03[a]
Normalized step length (step length/leg length)	0.96±0.09	0.96±0.08	0.96±0.09	0.96±0.09
Cadence (steps min^{-1})	118.3±7.29	124.6±10.5[a]	128.4±10.1[a,b]	128.4±10.6[a,b]
Braking phase (% stance phase)	52.1±4.46	44.3±4.98[a]	41.5±2.93[a,b]	38.3±2.92[a,b,c]

Values expressed as means±s.d. [a,b,c]Significant differences (P<0.05). RE, regular erect trunk; TF1, 30 deg trunk flexion; TF2, 50 deg trunk flexion; TF3, maximal trunk flexion.

governed simply by:

$$F_a = k_p(l_0 - l) + c_p\dot{l}, \quad (1)$$

where l and $\dot{l}$ are the instantaneous length and the rate of length change of the leg, respectively, k_p is the stiffness of the parallel spring, l_0 the rest length of the leg and c_p<0 the damping parameter of the parallel damper. The first term of the sum is the contribution of the spring and the right term is the contribution of the damper to axial force.

For the serial arrangement, F_a is equal in the spring and the damper, and the sum of the length of the spring l_s and the distance the damper travelled l_d equals l. Thus, the force is given by:

$$F_a = k_s(l_{s0} - l_s) = c_s\dot{l}_d\,, \quad (2)$$

where k_s and l_{s0} are the stiffness and rest length of the serial spring, c_s<0 and $\dot{l}_d$ are the damping parameter and the rate of length change of the serial damper, respectively. Hence, l_d can be obtained by integration of:

$$\dot{l}_d = \frac{k_s}{c_s}\cdot(l_{s0} - l + l_d). \quad (3)$$

In simulations, the initial length of the damper was set to zero.

Optimization

We minimized the sum of squared differences between the axial force that our leg models produced and the measured axial force by varying the independent spring and damper parameters with the MATLAB algorithm GlobalSearch. The leg length–time data were used as input. In both leg models, the rest lengths of the springs were dependent parameters. They were chosen such that the models reproduced the force at TD. We set lower bounds and upper bounds for stiffness and damping values. Stiffness values did not reach boundaries, yet damping values did reach upper (0 N s m^{-1}) and lower bounds (−100,000 N s m^{-1}) in some cases (especially in upright walking) for the PSD and the SSD model, respectively. For the PSD model, a damping value of 0 N s m^{-1} indicates that the

Table 2. Kinetic and kinematic parameters

	RE	TF1	TF2	TF3
Kinematics				
$Trunk_{TD}$ (deg)	7.70±3.08	32.4±7.20[a]	47.2±6.30[a,b]	71.7±7.80[a,b,c]
$Trunk_{TO}$ (deg)	5.70±2.90	30.9±6.47[a]	47.6±7.54[a,b]	71.3±7.16[a,b,c]
$Trunk_{RoM}$ (deg)	3.37±1.49	7.37±3.75[a]	9.09±2.90[a,b]	7.28±2.04[a,c]
$Trunk_{max}$ (deg)	8.25±3.09	34.5±6.76[a]	51.5±7.23[a,b]	77.1±7.03[a,b,c]
Hip_{TD} (deg)	20.7±4.38	41.7±8.08[a]	55.0±8.16[a,b]	77.1±7.27[a,b,c]
Hip_{TO} (deg)	−14.4±6.13	10.9±10.8[a]	23.5±9.50[a,b]	49.8±9.11[a,b,c]
Hip_{RoM} (deg)	41.2±3.24	39.4±4.14	37.5±4.95[a]	33.9±5.79[a,b,c]
Hip_{max} (deg)	24.9±5.12	47.6±7.81[a]	60.1±7.92[a,b]	83.1±5.73[a,b,c]
$Knee_{TD}$ (deg)	9.32±4.24	10.1±3.87	10.9±5.24	13.6±6.23[a,b,c]
$Knee_{TO}$ (deg)	35.1±5.49	40.2±6.20[a]	45.2±6.51[a,b]	54.02±8.31[a,b,c]
$Knee_{RoM}$ (deg)	68.3±3.56	66.6±2.78[a]	67.1±3.07	67.4±3.71
$Knee_{max}$ (deg)	74.8±3.11	74.4±4.03	75.4±4.99	79.4±8.03[a,b,c]
$Ankle_{TD}$ (deg)	−1.17±2.13	2.16±2.29[a]	2.15±2.97[a]	2.42±3.36[a]
$Ankle_{TO}$ (deg)	−11.2±5.69	−6.81±5.11[a]	−4.46±5.18[a,b]	−2.67±6.41[a,b]
$Ankle_{RoM}$ (deg)	36.3±6.54	29.9±4.77[a]	27.8±4.62[a]	28.7±4.63[a]
Ankle dorsiflexion (deg)	7.25±4.43	8.45±4.25	9.68±4.57[a]	12.6±5.17[a,b,c]
Ankle plantarflexion (deg)	−29.1±7.76	−21.5±5.76[a]	−18.1±4.90[a,b]	−21.2±7.69[a,b]
CoM_{TD} (m)	0.87±0.47	0.84±0.39	0.84±0.44[a]	0.78±0.66[a,b,c]
CoM_{TO} (m)	0.87±0.43	0.84±0.36[a]	0.83±0.48[a]	0.79±0.61[a,b,c]
CoM_{RoM}* (m)	0.03±0.01	0.04±0.01[a]	0.03±0.01[b]	0.03±0.01
CoM_{max}* (m)	0.89±0.04	0.87±0.03[a]	0.86±0.04[a]	0.8±0.05[a,b,c]
Kinetic data				
V_{GRF1} (N BW^{-1})	1.21±0.82	1.33±0.14[a]	1.39±0.40[a,b]	1.38±0.15[a]
V_{GRF2} (N BW^{-1})	1.15±0.07	0.97±0.10[a]	0.89±0.11[a,b]	0.87±0.09[a,b]
H_{GRFb} (N BW^{-1})	−0.21±0.05	−0.25±0.08[a]	−0.28±0.09[a]	−0.31±0.10[a,b]
H_{GRFp} (N BW^{-1})	0.26±0.03	0.24±0.03[a]	0.22±0.04[a,b]	0.21±0.04[a,b]
I_S	1.86±0.12	1.76±0.15[a]	1.70±0.14[a,b]	1.71±0.14[a,b]

Values are expressed as means±s.d. [a,b,c]Significant differences (P<0.05). RE, regular erect trunk; TF1, 30 deg trunk flexion; TF2, 50 deg trunk flexion; TF3, maximal trunk flexion; TD, touchdown; TO, toe-off; RoM, range of motion; max, maximal; V_{GRF1}, 1st peak of vertical ground reaction force; V_{GRF2}, 2nd peak of vertical ground reaction force; H_{GRFb}, peak horizontal braking force; H_{GRFp}, peak horizontal propulsive force; I_S, dimensionless vertical or support impulse.
*: measured during stance phase.

Journal of Experimental Biology (2017) 220, 478-486 doi:10.1242/jeb.148312

Table 3. Leg parameters obtained from experimental data

	RE	TF1	TF2	TF3
Normalized leg length (TD)	1.14±0.35	1.15±0.03	1.15±0.03	1.14±0.03
Normalized leg length (TO)	1.11±0.07	1.1±0.35	1.09±0.35[a]	1.06±0.35[a,b,c]
α_{TD}	66.1±4.67	63.6±4.49[a]	63.4±4.58[a]	62.9±4.74[a]
α_{TO}	116.3±3.38	113.9±3.25[a]	113.9±3.31[a]	112.5±3.62[a,b]

α_{TD}, angle of attack; α_{TO}, leg orientation at TO. Values expressed as means±s.d. [a,b,c]Significant differences (P<0.05). RE, regular erect trunk; TF1, 30 deg trunk flexion; TF2, 50 deg trunk flexion; TF3, maximal trunk flexion.

damper produces no force, and for the SSD model, a damping value of −100,000 Ns m^{-1} means that the damper barely moved. In both cases, the PSD and the SSD leg models are in effect reduced to a spring. To compare the quality of the fit between PSD and SSD models, we used the root mean square (RMS) values that were normalized to the maximal axial force of each trial.

RESULTS

Spatiotemporal parameters

Group means and standard deviations for spatiotemporal gait parameters are listed in Table 1. Except for normalized step length, significant differences (P<0.05) were found across gait conditions for the entire gait parameters. As trunk flexion angle increased, an upward trend can be observed in the velocity and cadence, and a downward trend in the stance time and swing time. Between TF2 and TF3, there were no significant differences in parameters.

Joint kinematics

Fig. 2A shows the mean pattern of the trunk angle across gait conditions throughout the gait cycle. The joint kinematics parameters are shown in Table 2 (classified by postures). When clustering by posture, differences (P<0.05) among groups were found for all parameters of interest. Not surprisingly, the greater the trunk flexion, the larger the hip flexion angle at TD and TO, and the greater the peak hip flexion angle during the gait cycle. The hip range of motion decreased with trunk flexion (Fig. 2B, Table 2).

Knee flexion at TD and TO as well as peak knee flexion increased with trunk flexion. In contrast, the knee range of motion decreased marginally with trunk flexion (Fig. 2C, Table 2).

With increased trunk flexion, the ankle tended to be significantly more dorsiflexed at TD and less plantarflexed at TO (Table 2). Also, the peak ankle dorsiflexion during stance increased while the peak ankle plantarflexion during swing was lower for gaits with a trunk-flexed posture.

The vertical position of the CoM at TO was nearly the same as that at TD within each gait condition (Fig. 3). However, compared with RE, the vertical position of CoM at TD and TO decreased significantly by ∼10% in TF3 (Fig. 3C, Table 2).

Kinetic parameters

Fig. 3 shows the average normalized vertical (A) and anterior–posterior (B) GRFs at the preferred walking speed for the different trunk-flexed postures. Although the magnitude of V_{GRF1} was significantly higher for trunk-flexed postures, V_{GRF2} decreased with trunk flexion by up to 24% in TI3 gait (Table 2). In comparison to regular erect trunk (RE) gait, H_{GRFb} amplitude increased by up to 47% and H_{GRFp} amplitude decreased by up to 19% in TF3 (Fig. 3A, Table 2). These resulted in a more asymmetric profile of vertical GRFs, with the second peaks and valley much less pronounced for trunk-flexed postures and asymmetric profile of horizontal GRFs, with higher H_{GRFb} and lower H_{GRFp} (Fig. 3). Moreover, with increased trunk flexion, the braking phase was systematically decreased by ∼26% in TF3 gait (Table 2). The support impulse

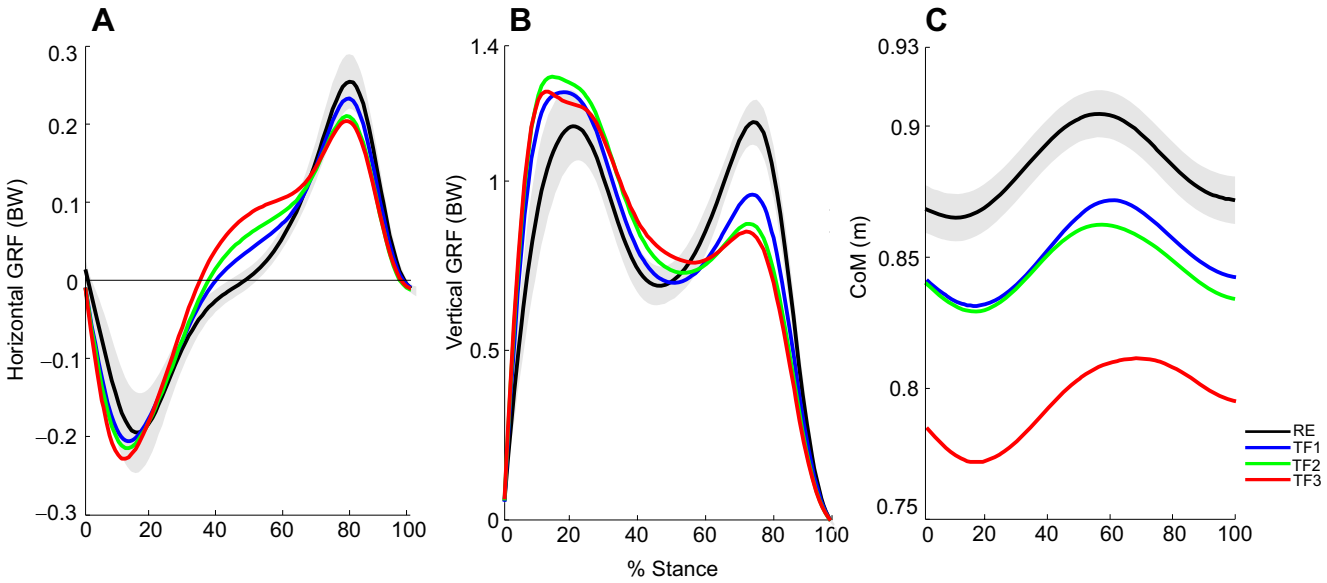

Fig. 3. Ground reaction forces (GRF) and CoM waveforms for different walking conditions. Shown are ensemble-averaged horizontal GRF (A), vertical GRF (B) [normalized to participant body weight (BW)] and centre of mass (CoM) (C) for RE, TF1, TF2 and TF3 level walking gaits during the stance phase (N=12). The contact time is normalized to 100%. The grey shaded area represents the corresponding s.d. RE, regular erect trunk; TF1, 30 deg trunk flexion; TF2, 50 deg trunk flexion; TF3, maximal trunk flexion.

Journal of Experimental Biology

Journal of Experimental Biology (2017) 220, 478-486 doi:10.1242/jeb.148312

decreased significantly from 1.86±0.12 in RE by ∼5% to 1.76±0.12 in TF1 and 8% to 1.7±0.14 in TF2 and TF3, respectively (Table 2).

Properties of the leg

Table 3 lists the group mean±s.d. values pertaining to the properties of the leg across gait postures. Participants showed adaptations in the leg angle at TD (α_{TD}) and TO (α_{TO}) for the different trunk angles (Table 3). The leg angle decreased significantly by 4.8% from 66.1±4.67 deg (RE) to 62.9±4.74 deg(TF3) at TD and by 3.2% from 116.3±3.38 deg (RE) to 112.5±3.62 deg (TF3) at TO. In other words, during maximal trunk-flexed gait, the leg displayed a flatter angle at TD and a steeper angle at TO.

The leg length at TD remained almost unaffected (P=0.514), whereas the leg length at TO significantly decreased across postures with increased trunk flexion angle (P<0.001). The leg length exhibited a strong asymmetry during the stance phase (longer at TD and shorter at TO; Fig. 4A, Table 3).

The SSD model produced significantly better predictions of leg axial forces than the PSD model for trunk-flexed gaits (Fig. 5, Fig. 6). The SSD model fitted axial force in TF2 better than in other gait conditions (Fig. 5C). The average deviation of the SSD model force from axial force was 0.16 (RE), 0.11 (TF1), 0.1 (TF2) and 0.13 (TF3) of the maximal force.

DISCUSSION

An increase of sagittal trunk flexion led to greater kinetic and kinematic intra-limb asymmetries (Figs 3 and 4). Despite the considerable differences in leg morphology and size between humans and birds, able-bodied walking with maximum trunk flexion (TF3) produces a leg function similar to that found in birds. Moreover, for all trunk angles, the leg model with spring and damper in series gives a superior prediction of the axial leg function (Figs 5 and 6).

The findings of the current study support the hypothesis that the sagittal trunk posture leads to altered gait parameters and leg function. Specifically, it was hypothesized that changes in trunk orientation would result in right-skewed vertical GRF profiles and in shorter duration of braking relative to the propulsion phase. Compared with RE gait, vertical GRF tended to be more asymmetric with increasing trunk flexion (Fig. 3B). In contrast to the symmetric, M-shaped vertical GRF pattern during RE gait in humans, vertical GRF approximated the right-skewed profile found in birds with pronograde trunk orientation (Andrada et al., 2014). Furthermore, the duration of the braking phase decreased significantly with trunk flexion (Fig. 3A, Table 2) towards values found in birds (Andrada et al., 2014). These dynamic similarities between bird and human trunk-flexed locomotion suggest that the trunk configuration causes these dynamic asymmetries and that the leg (connecting hip and CoP) operation is independent of the specific leg morphology.

While the normalized length of the leg remained unchanged at TD, with increasing trunk flexion it underwent a significant decrease at TO. Together with the posterior shift of the pelvis, the unchanged leg length at TD led to a decrease in the distance between the CoM and the CoP. In order to prevent toppling or falling over, TO occurred at a steeper angle in the trunk-flexed gait. To maintain a sufficient step length, the posterior shift of the pelvis is compensated in part by choosing a flatter angle of attack (leading to a ∼0.02 m gain in TD position). Still, step time in trunk-flexed walking remained shorter than in the RE gait, which is also reflected in a significant decrease of support impulse (Table 2). Consequently, the braking phase became shorter relative to the propulsion phase with an increase of trunk flexion, suggesting that the average braking force must be larger than the average propulsive force to yield zero impulse in horizontal direction, i.e. to keep locomotion speed constant. Assuming that an increase in propulsive force is associated with increased axial leg force, the reduced braking time (Table 2) leads to the right-skewed vertical GRF profile.

Walking with bent postures was associated with a crouched gait pattern, characterized by a sustained knee flexion throughout the stance phase, and an increase in hip flexion and ankle dorsiflexion (Wren et al., 2005; Saha et al., 2008). This can be explained with a flatter angle of attack that leads to a decreased height of the hip above the ground, which in turn yields more flexed limb joints during trunk-flexed walking. In addition, with increasing trunk flexion, the angular range of motion decreased across lower limb joints (Table 2) because in more flexed limbs, smaller angular

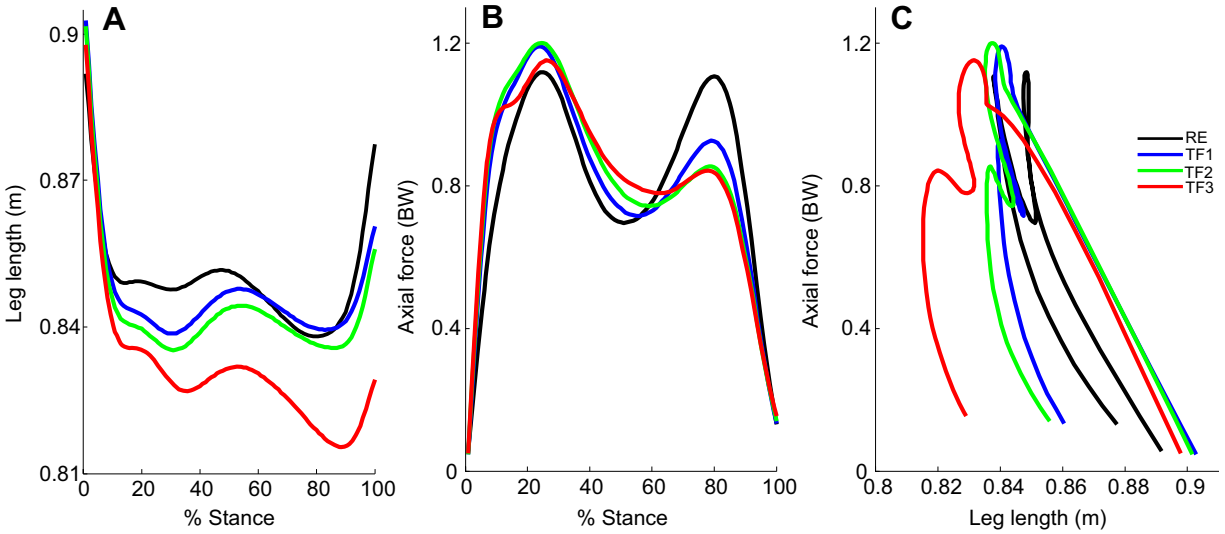

Fig. 4. Axial leg function. Averaged (A) leg length, (B) axial leg force and (C) axial loop (axial force versus leg length) for RE and, TF1, TF2 and TF3 gaits (N=12). Axial loops start at long length and end with a shorter leg length (counterclockwise loop). The contact time is normalized to 100%. RE, regular erect trunk; TF1, 30 deg trunk flexion; TF2, 50 deg trunk flexion; TF3, maximal trunk flexion.

Journal of Experimental Biology (2017) 220, 478-486 doi:10.1242/jeb.148312

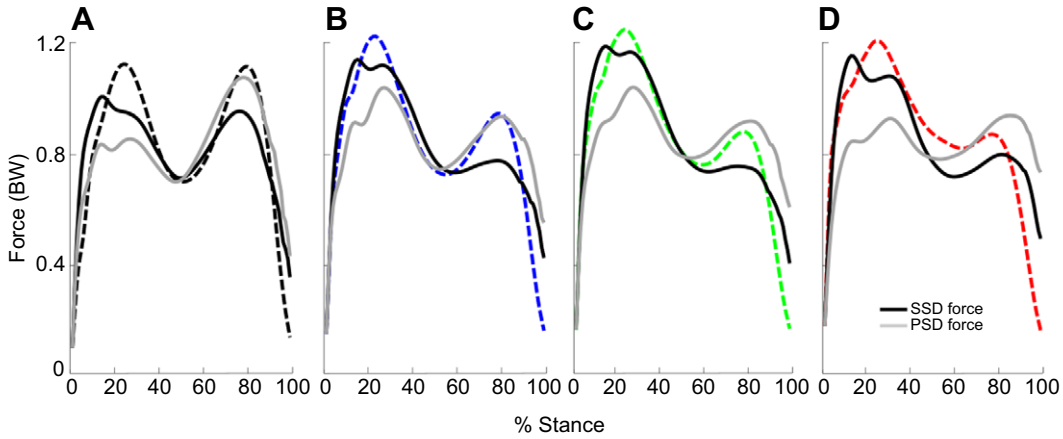

Fig. 5. Model forces versus experimental axial force for different walking conditions. (A) RE, (B) TF1, (C) TF2 and (D) TF3 gaits (*N*=12). Shown are normalized ensemble-averaged leg axial force (dashed lines), fit from SSD model (series-spring-damper, solid black curve) and fit from PSD model (parallel-spring-damper, solid grey curve). SSD model produces better predictions of leg axial forces in response to trunk-flexed postures than the PSD model across all gait conditions (Fig. 6). RE, regular erect trunk; TF1, 30 deg trunk flexion; TF2, 50 deg trunk flexion; TF3, maximal trunk flexion.

changes are required to achieve similar leg length changes to those measured in upright walking with extended legs. Since locomotion with trunk-flexed postures was achieved by bending over at the waist, the hip joint showed the greatest extent of flexion throughout the gait cycle in comparison to RE gait (Table 2). With increasing sagittal trunk flexion, all leg joints were flexed more at TO owing to the earlier TO at a steeper angle (Table 2). The kinematic asymmetries in trunk-flexed gait (TD and TO angles and leg lengths) are in agreement with those found in birds (Andrada et al., 2014).

Compared with RE walking, in our study, walking with maximal trunk flexion (TF3) led to ∼10% greater self-selected gait velocity and cadence, ∼10% shorter stance time and ∼5% shorter swing duration while the normalized step length remained unchanged. In our experiment, the task of foot strikes in left–right–left sequence on three equidistant force plates embedded in the walkway may have prompted the participants to maintain constant step lengths. With the same step lengths and lower vertical impulse per step, a higher cadence is necessary to support the body weight. This in turn enforces higher speed. Such increased walking speed is not in agreement with the result observed by Saha et al. (2008), who found that walking speed does not significantly vary during walking with trunk-flexed postures. The reason for this inconsistency may be attributed to different approaches employed to control the trunk postures. They used a program that allows continuous, real time estimation of the trunk flexion angle via provision of auditory cues, which may have required participants to walk slower in order to maintain their trunk close to the desired angle. In contrast, in our experiments the trunk angle was checked visually by an independent examiner, which may have led to less constrained walking conditions.

It may be speculated that the imposed trunk flexion in TF1 and TF2 would limit the range of angular excursion throughout the gait. In contrast, trunk excursions were increased in trunk-flexed gaits compared with RE gait (Fig. 2A, Table 2). Owing to the posterior shift of the hip in the forward bent posture, the horizontal leverage of the CoM with respect to the hip is increased. After TD, the zig-zag configuration of the leg and body responds with bending (Fig. 2). In addition, an increased first peak of the ground reaction force increases the impulse in the first half of the contact. This is accompanied by increased hip muscle forces necessary to balance trunk weight in a more bent posture. These increased forces can, in part, be achieved by a stronger recruitment and by higher passive forces due to elongation of hip muscles that would contribute to muscular compliance and hence to oscillations. This argument can, however, not explain the relatively similar range of motion of the trunk angle for all trunk-flexed gaits (Table 2).

Kluger et al. (2014) analysed in detail the kinetics and energetics of lower limb joints in the context of trunk-flexed walking. They reported increased hip extension torques and hip work, and

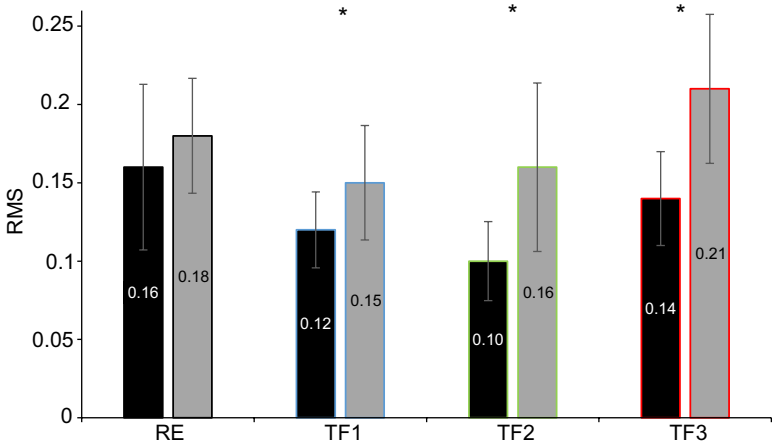

Fig. 6. Root mean square (RMS) difference between model forces and experimental axial force. Shown are ensemble-averaged RMS obtained by nonlinear curve fitting using SSD model (series-spring damper, black) and PSD model (parallel-spring damper, grey) for the gait conditions RE, TF1, TF2 and TF3. Error bars denote s.d.; asterisks denote statistically significant differences across conditions. Mean RMS values for SSD model were significantly lower than those for SSD model across all gait conditions except for RE gait (RE: t_{11}=1.54, P=0.174; TF1: t_{11}=3.21, P=0.008; TF2: t_{11}=3.69, P=0.004; TF3: t_{11}=4.95, P<0.001). RE, regular erect trunk; TF1, 30 deg trunk flexion; TF2, 50 deg trunk flexion; TF3, maximal trunk flexion.

Journal of Experimental Biology

decreased plantarflexion torques and negative work at the ankle joint during stance phase. In a recent work, Blickhan et al. (2015) investigated the effect of the hip placement directly below, at, or above the virtual pivot point (intersection of GRFs above CoM). They revealed that shifting the hip far posteriorly, as observed in some birds, can lead to the production of pure extension torques throughout the stance phase. These results are consistent with large hip torques and positive work at the hip and negative work at the tarsometatarsal–phalangeal joint – the functional equivalent of the ankle joint – in birds (Cavagna et al., 1963). In accordance with the increased energy dissipation in the ankle joint, our results show that energy dissipation in the leg in the axial direction increases with the increase of trunk flexion angle (Fig. 4C). Therefore, the relative placement of the hip with respect to the CoM is proposed to be an important measure in the modifications of leg function, and consequently, for balancing the trunk in legged motion systems (Blickhan et al., 2015).

The model with a spring in series with the damper produced better predictions of the leg forces than the parallel spring-damper model across all trunk-flexed gaits (Figs 5 and 6). Interestingly, in the case of RE walking, for both models, in many cases the optimization yielded parameters that corresponded to spring-like leg behaviour with negligible energy dissipation, and the model predictions were not significantly different (Fig. 6). This indicates that the damper does not substantially improve the reproduction of the human leg forces in walking with upright trunk, which corroborates the assumption of spring-like leg behaviour in conceptual models of human walking (Geyer et al., 2006). Although the parallel spring and damper model has been widely used in biomechanics and robotics to describe and investigate legged locomotion (Shen and Seipel, 2012; Andrada et al., 2014), our results highlight that the serial spring and damper model is superior in predictions of axial leg force of trunk-flexed walking. Because the leg models differ in their dynamic responses, we argue that employing the spring in series with the damper model may yield altered predictions of the locomotion stability in birds.

Understanding the interaction between posture and hip arrangement and their relation to axial leg function may be relevant in the medical field, in engineering and in explaining the evolution of a bipedal gait. For example, the observed intra-limb asymmetries as a consequence of trunk-flexed posture and associated compensatory mechanisms may be of clinical relevance for patients exhibiting a disordered gait (Saha et al., 2008; Doherty et al., 2011; de Groot et al., 2014). Engineers designing not merely androids but also robot birds and other creatures (Hyon et al., 2003; Hugel et al., 2011; Zhou and Bi, 2012) may benefit from the characterization of the axial leg function and its modelling e.g. for trajectory planning in virtual model control of bipedal robotic locomotion (Sreenath et al., 2011). Last, but not least, based on the differences in body size and limb morphology, the comparison of living avian and human bipeds may facilitate the interpretation of the evolution of bipedal locomotion (Gatesy and Biewener, 1991; Hirasaki et al., 2004; Schwartz, 2007; Thorpe et al., 2007; Foster et al., 2013).

The results of this study highlight the effects of sagittal trunk orientation on leg function in bipeds and reveals that the spring and damper in series model is superior in the reproduction of axial leg function in trunk-flexed gaits. An experimentally prescribed pronograde posture in able-bodied walking induces asymmetries in leg function characterized by a right-skewed vertical GRF and a shorter leg length at TO, which are similar to the asymmetries found in birds. Considering these similarities in locomotion between bird and human with trunk flexed, we conclude that the necessity to stabilize the trunk constrains the basic leg function independent of the specific leg morphology, at least in the investigated species.

Acknowledgements
Authors thank Johanna Vielemeyer for her valuable contribution to collecting experimental data.

Competing interests
The authors declare no competing or financial interests.

Author contributions
The experiments were planned by R.B., supervised by R.M., and carried out by S.A. The data were analysed by S.A. and C.R. All authors contributed to the interpretation of the results and revised the manuscript.

Funding
This research received no specific grant from any funding agency in the public, commercial or not-for-profit sectors.

References
Alexander, R. M. N. (1991). Energy-saving mechanisms in walking and running. *J. Exp. Biol.* **160**, 55-69.
Alexander, R. M. N. (2004). Bipedal animals, and their differences from humans. *J. Anat.* **204**, 321-330.
Andrada, E., Rode, C., Sutedja, Y., Nyakatura, J. A. and Blickhan, R. (2014). Trunk orientation causes asymmetries in leg function in small bird terrestrial locomotion. *Proc. Biol. Sci.* **281**.
Blickhan, R., Andrada, E., Müller, R., Rode, C. and Ogihara, N. (2015). Positioning the hip with respect to the COM: Consequences for leg operation. *J. Theor. Biol.* **382**, 187-197.
Cavagna, G. A., Saibene, F. P., Santi, G. F. and Margaria, R. (1963). Analysis of the mechanics of locomotion. *Exp. Med. Surg.* **21**, 117-126.
de Groot, M. H., van der Jagt-Willems, H. C., van Campen, J. P. C. M., Lems, W. F., Beijnen, J. H. and Lamoth, C. J. C. (2014). A flexed posture in elderly patients is associated with impairments in postural control during walking. *Gait Posture* **39**, 767-772.
de Leva, P. (1996). Adjustments to Zatsiorsky-Seluyanov's segment inertia parameters. *J. Biomech.* **29**, 1223-1230.
Dingwell, J. B., John, J. and Cusumano, J. P. (2010). Do humans optimally exploit redundancy to control step variability in walking? *PLoS Comput. Biol.* **6**, e1000856.
Doherty, K. M., van de Warrenburg, B. P., Peralta, M. C., Silveira-Moriyama, L., Azulay, J.-P., Gershanik, O. S. and Bloem, B. R. (2011). Postural deformities in Parkinson's disease. *Lancet Neurol.* **10**, 538-549.
Foster, A. D., Raichlen, D. A. and Pontzer, H. (2013). Muscle force production during bent-knee, bent-hip walking in humans. *J. Hum. Evol.* **65**, 294-302.
Gard, S. A., Miff, S. C. and Kuo, A. D. (2004). Comparison of kinematic and kinetic methods for computing the vertical motion of the body center of mass during walking. *Hum. Mov. Sci.* **22**, 597-610.
Gatesy, S. M. and Biewener, A. A. (1991). Bipedal locomotion: effects of speed, size and limb posture in birds and humans. *J. Zool.* **224**, 127-147.
Geyer, H., Seyfarth, A. and Blickhan, R. (2003). Positive force feedback in bouncing gaits? *Proc. Biol. Sci.* **270**, 2173-2183.
Geyer, H., Seyfarth, A. and Blickhan, R. (2006). Compliant leg behaviour explains basic dynamics of walking and running. *Proc. R. Soc. B Biol. Sci.* **273**, 2861-2867.
Gillet, C., Duboy, J., Barbier, F., Armand, S., Jeddi, R., Lepoutre, F.-X. and Allard, P. (2003). Contribution of accelerated body masses to able-bodied gait. *Am. J. Phys. Med. Rehabil.* **82**, 101-109.
Grasso, R., Zago, M. and Lacquaniti, F. (2000). Interactions between posture and locomotion: motor patterns in humans walking with bent posture versus erect posture. *J. Neurophysiol.* **83**, 288-300.
Gundersen, L. A., Valle, D. R., Barr, A. E., Danoff, J. V., Stanhope, S. J. and Snyder-Mackler, L. (1989). Bilateral analysis of the knee and ankle during gait: an examination of the relationship between lateral dominance and symmetry. *Phys. Ther.* **69**, 640-650.
Herzog, W., Nigg, B. M., Read, L. J. and Olsson, E. (1989). Asymmetries in ground reaction force patterns in normal human gait. *Med. Sci. Sports Exerc.* **21**, 110-114.
Hirasaki, E., Ogihara, N., Hamada, Y., Kumakura, H. and Nakatsukasa, M. (2004). Do highly trained monkeys walk like humans? A kinematic study of bipedal locomotion in bipedally trained Japanese macaques. *J. Hum. Evol.* **46**, 739-750.
Hof, A. L. (1996). Scaling gait data to body size. *Gait Posture* **4**, 222-223.
Hugel, V., Hackert, R. and Abourachid, H. (2011). Kinematic modeling of bird locomotion from experimental data. *IEEE Trans. Robot.* **27**, 185-200.
Hutchinson, J. R. and Allen, V. (2009). The evolutionary continuum of limb function from early theropods to birds. *Naturwissenschaften* **96**, 423-448.

Hyon, S., Emura, T. and Mita, T. (2003). Dynamics-based control of a one-legged hopping robot. *J. Syst. Control Eng.* **217**, 83-98.
Kluger, D., Major, M. J., Fatone, S. and Gard, S. A. (2014). The effect of trunk flexion on lower-limb kinetics of able-bodied gait. *Hum. Mov. Sci.* **33**, 395-403.
Leteneur, S., Gillet, C., Sadeghi, H., Allard, P. and Barbier, F. (2009). Effect of trunk inclination on lower limb joint and lumbar moments in able men during the stance phase of gait. *Clin. Biomech.* **24**, 190-195.
Leteneur, S., Simoneau, E., Gillet, C., Dessery, Y. and Barbier, F. (2013). Trunk's natural inclination influences stance limb kinetics, but not body kinematics, during gait initiation in able men. *PLoS ONE* **8**, e55256.
Maus, H. M., Lipfert, S. W., Gross, M., Rummel, J. and Seyfarth, A. (2010). Upright human gait did not provide a major mechanical challenge for our ancestors. *Nat. Commun.* **1**, 70.
McGibbon, C. A. and Krebs, D. E. (2001). Age-related changes in lower trunk coordination and energy transfer during gait. *J. Neurophysiol.* **85**, 1923-1931.
McMahon, T. A., Valiant, G. and Frederick, E. C. (1987). Groucho running. *J Appl Physiol. (1985)* **62**, 2326-2337.
Merker, A., Rummel, J. and Seyfarth, A. (2011). Stable walking with asymmetric legs. *Bioinspir. Biomim.* **6**, 045004.
Müller, R., Tschiesche, K. and Blickhan, R. (2014). Kinetic and kinematic adjustments during perturbed walking across visible and camouflaged drops in ground level. *J. Biomech.* **47**, 2286-2291.
Müller, R., Birn-Jeffery, A. V. and Blum, Y. (2016). Human and avian running on uneven ground: a model-based comparison. *J R Soc. Interface* **13**.
Sadeghi, H., Allard, P., Prince, F. and Labelle, H. (2000). Symmetry and limb dominance in able-bodied gait: a review. *Gait Posture* **12**, 34-45.
Saha, D., Gard, S. and Fatone, S. (2008). The effect of trunk flexion on able-bodied gait. *Gait Posture* **27**, 653-660.
Schwartz, J. H. (2007). The origins of human bipedalism. *Science* **318**, 1065; author reply 1065.
Shen, Z. H. and Seipel, J. E. (2012). A fundamental mechanism of legged locomotion with hip torque and leg damping. *Bioinspir. Biomim.* **7**, 046010.
Sreenath, K., Park, H.-W., Poulakakis, I. and Grizzle, J. W. (2011). A compliant hybrid zero dynamics controller for stable, efficient and fast bipedal walking on MABEL. *Int. J. Robot. Res.* **30**, 1170-1193.
Thorpe, S. K. S., Holder, R. L. and Crompton, R. H. (2007). Origin of human bipedalism as an adaptation for locomotion on flexible branches. *Science* **316**, 1328-1331.
Toda, H., Nagano, A. and Luo, Z. (2015). Age and gender differences in the control of vertical ground reaction force by the hip, knee and ankle joints. *J. Phys. Ther. Sci.* **27**, 1833-1838.
Winiarski, S. and Rutkowska-Kucharska, A. (2009). Estimated ground reaction force in normal and pathological gait. *Acta Bioeng. Biomech.* **11**, 53-60.
Wren, T. A., Rethlefsen, S. and Kay, R. M. (2005). Prevalence of specific gait abnormalities in children with cerebral palsy: influence of cerebral palsy subtype, age, and previous surgery. *J. Pediatr. Orthop.* **25**, 79-83.
Zhou, X. and Bi, S. (2012). A survey of bio-inspired compliant legged robot designs. *Bioinspir. Biomim.* **7**, 041001.